Characteristics of Drug–Phospholipid Coprecipitates I: Physical Properties and Dissolution Behavior of Griseofulvin–Dimyristoylphosphatidylcholine Systems

S. VENKATARAM and J. A. ROGERS ˣ

Received February 24, 1983, from the *Faculty of Pharmacy and Pharmaceutical Sciences, University of Alberta, Edmonton, Alberta, Canada.* Accepted for publication May 11, 1983.

Abstract □ Solid dispersions of griseofulvin and dimyristoylphosphatidylcholine (lecithin) have been prepared as both coprecipitates and physical mixtures, and their physical characteristics and dissolution behavior compared with pure griseofulvin. The dissolution of the physical mixtures was similar to pure drug, but the coprecipitates yielded a 3.5-fold greater initial dissolution rate and a limiting concentration after 60 min which was 72% greater at a griseofulvin–lecithin weight ratio of 19:1. Increasing the lecithin content to 1.5:1 compositions resulted in only a further 50% increase in the initial dissolution rate and a further 12% increase in the limiting concentration. The effect of the pH of the medium on dissolution was slight, but varied with the composition of the system. The phase diagram indicated that these systems have no significant eutectic or solid solution formation. X-ray diffraction spectra further showed that freshly prepared or aged coprecipitates contained griseofulvin crystals, and photomicrographs showed that the crystals essentially retained their characteristic shapes and sizes in all systems. Differential thermal analysis yielded heats of fusion that gave a good linear correlation with the percent of griseofulvin dissolved from coprecipitates at all time intervals, but not with physical mixtures. Furthermore, aged coprecipitates underwent a slower rate of dissolution compared with fresh samples. The results are interpreted to suggest that griseofulvin undergoes improved dissolution from coprecipitates due to the formation of crystals of lower stability. In addition, the rapid dispersion of lecithin in the aqueous medium (as seen microscopically) entraps griseofulvin in myelinic structures and liposomes and effectively increases the saturation concentration of drug in the diffusion layer during the dissolution process.

Keyphrases □ Drug–phospholipid coprecipitates—griseofulvin–dimyristoylphosphatidylcholine system, dissolution behavior, physical properties □ Dissolution—griseofulvin–dimyristoylphosphatidylcholine coprecipitates, comparison with physical mixtures, physical properties □ Griseofulvin—coprecipitates with dimyristoylphosphatidylcholine, physical properties, dissolution behavior

The dissolution of solid drugs having low water solubility is often a rate-limiting step in obtaining bioavailability. Thus, several formulation approaches have been explored to improve bioavailability of such drugs, including the use of lipid vehicles and the preparation of solid dispersions. In those cases where lipids have been used, the dissolution and bioavailability of drugs have been found to be dependent on the nature of the lipids used in the formulation, being either increased (1–4), decreased (1, 3–5), or unaffected (1). In most instances, the dosage form contains a large proportion of lipid. Likewise, solid dispersions involving water-soluble carriers require a large proportion of carrier to be effective. On the other hand, it would be advantageous to incorporate a minimal amount of carrier to produce either rapid dissolution or sustained release of a drug from a solid dosage form.

Phospholipids spontaneously disperse in aqueous media to form bilayer structures which have the capacity to entrap or sequester solutes. This dual behavior could prove beneficial for improving bioavailability of drugs in a number of ways. According to the Nernst film theory of dissolution, an increased saturation concentration of drug in the stationary layer leads to an increase in the dissolution rate. It is not important that the concentration achieved is due to the intrinsic solubility of the drug in the medium of the stationary layer or due to a partitioning process. Encapsulated or entrapped drug within the bilayer structures (myelinic or liposomal) during the dissolution process may be transported, first to the stationary or diffusion layer, then to the bulk solution, then to the site of absorption to yield rapid delivery of a drug to the general circulation. Furthermore, for drugs which may be susceptible to degradation or solubility changes within the GI fluids, entrapment may afford a degree of protection (6, 7).

The system of griseofulvin–dimyristoylphosphatidylcholine has been chosen to test these hypotheses and to evaluate the performance of a phospholipid in a solid dispersion formulation. The purpose of the present report is to present some preliminary data for this system and to evaluate its potential in controlled-release dosage form design.

EXPERIMENTAL

Materials—Micronized griseofulvin[1] (I) was pretreated by dissolving it in chloroform then removing the solvent by warming slightly over a water bath and applying a gentle stream of air. Drying of the crystals was carried out under vacuum over desiccants. The melting points of untreated and treated I were identical. Pure I and all binary mixtures were passed through an 80-mesh sieve[2] prior to testing.

L-α-Dimyristoylphosphatidylcholine[3] (II), claimed to be 98% pure, was used as received. All solvents and chemicals were reagent grade, and distilled water was used to prepare the dissolution media.

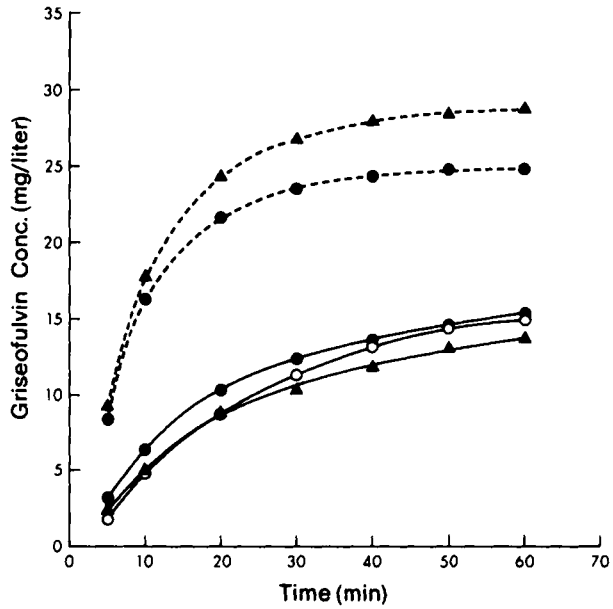

Figure 1—*Dissolution behavior of I and I–II solid dispersion systems at pH 2.0 and 37°C. Key: (- - -) coprecipitates; and (—) physical mixtures or pure I; (○) chloroform-treated I; (●) 9:1 composition of I–II; (▲) 1.5:1 composition of I–II.*

[1] Glaxo Canada Ltd., Toronto, Ontario.
[2] Standard (U.S. Series) sieve.
[3] Sigma Chemical Co., St. Louis, Mo.

0022-3549/84/0600-0757$01.00/0

Table I—Dissolution of Griseofulvin–Dimyristoylphosphatidylcholine Compositions at pH 2.0 and 37°C

Composition (Weight Ratio)	Initial Dissolution Rate, mg/L/min		Limiting Conc. After 60 min, mg/L	
	Coprecipitates	Physical Mixtures	Coprecipitates	Physical Mixtures
1:0	0.36	0.36	15.0	15.0
19:1	1.26	—	25.8	—
9:1	1.68	0.60	24.9	15.3
4:1	1.67	—	35.3	—
1.5:1	1.86	0.48	28.8	13.7

Preparation of Coprecipitates and Physical Mixtures—Solid dispersions of I–II compositions were prepared by the solvent method from chloroform, yielding coprecipitates which were subsequently dried under vacuum over desiccants as before. Coprecipitates were usually examined within 48 h after preparation. Physical mixtures were prepared by triturating appropriate quantities of I and II using a mortar and pestle, then transferring to a vacuum desiccator until ready for use.

Thermalmicroscopic Method—The thaw and melt temperatures of all samples were determined by the hot-stage microscopic technique[4]. The heating rate was set at 2°C/min. just below the predetermined thaw temperature.

Differential Thermal Analysis—The differential thermal analyzer[5] was calibrated with indium[6], tin[6], and lead[6] using a 15-mg sample against an empty pan as reference. The heating rate was set at 10°C/min, the differential temperature sensitivity was 0.3°C/2.54 cm, and the reference temperature sensitivity was 13.7°C/2.54 cm. Heats of fusion were determined from the areas under the endothermic peaks (planimeter method), and the corresponding calibration coefficients were obtained from the fusion temperatures (taken at the peak of the endothermic event) and the calibration curve (8).

X-ray Diffraction Studies—Samples for low-angle powder X-ray diffraction studies (~50 mg) were uniformly dispersed on a glass slide. A piece of transparent cellulose tape was then used to secure the powder in position. X-ray diffraction spectra[7] were obtained employing CuK_α radiation and run at 2°/min and a 2θ angle.

Dissolution Studies—The spin-filter dissolution test apparatus[8] employing a 1-μm porosity filter screen was used (9). Filter rotation speed was maintained at 600 rpm in 900 mL of dissolution medium, which was either HCl–KCl buffer at pH 2.0 or phosphate buffer at pH 5.0, at 37°C. Measurement of concentrations of I in the dissolution medium was carried out employing automated UV spectrometry at $\lambda = 293$ nm (10). A 50-mg sample was dispersed in the dissolution medium in each instance. The presence of II in the dissolution medium did not interfere with the analysis of I. Experiments were run in duplicate and the results averaged, although at no time was a significant difference found between duplicates.

Photomicrographic Analysis—Representative samples of powders were examined microscopically[9], 320× magnification, in either light mineral oil or water. Photomicrographs[10] were obtained for comparison of crystal shape and size and to record the various stages of dissolution.

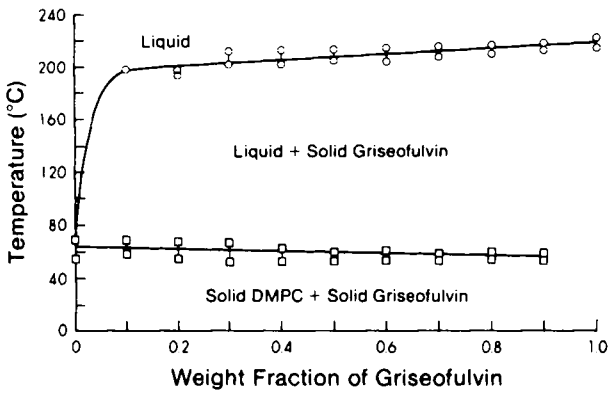

Figure 2—*Phase diagram of binary systems of I and II determined from differential thermal analysis and hot-stage microscopy. Key: (□) thaw and melt temperatures of the lower-melting component (II); (○) thaw and melt temperatures of the higher-melting component (I).*

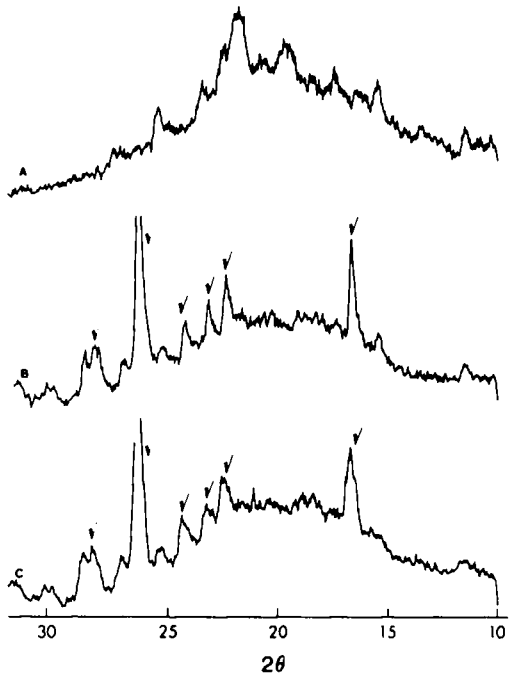

Figure 3—*Low angle powder X-ray diffraction spectra of II (A), chloroform-treated I (B), and 19:1, I–II coprecipitate (C).*

RESULTS

Dissolution Studies—The dissolution of I from a multiparticulate I–II coprecipitate was found to be considerably greater than from physical mixtures or pure I. Typical dissolution profiles are given in Fig. 1, where it is apparent that the initial dissolution rates and the amount of I dissolved after 60 min from the coprecipitates exceeded those of pure I or the corresponding physical mixtures. Furthermore, the dissolution of 1.5:1 coprecipitates was greater than that of the 9:1 composition, whereas the dissolution behavior of the corresponding physical mixtures was in the reverse order. The initial dissolution rates (IDR) (computed over the first 5 min of dissolution) and concentrations of I achieved after 60 min, which were essentially limiting after this period (LDC), are compared in Table I. The IDR of the I–II coprecipitate exhibits an increase of 3.5-fold with as little as 5% of II in the total sample (19:1 weight ratio) and an increase of 5-fold for samples containing 40% of II (1.5:1 weight ratio). In contrast, the IDR of I from physical mixtures increased only slightly with a higher content of II. Values of LDC obtained from coprecipitates clearly indicate a substantial increase in the apparent solubility of I in the dissolution medium. On the other hand, an increased fraction of II in the physical mixture compositions does not increase the apparent solubility of I and, indeed, at 40% II the LDC is somewhat lower than that for pure I. The superior dissolution of I–II coprecipitates is further exemplified by the data in Table II. Percent dissolved of I from coprecipitates is more than twice that dissolved from physical mixtures at corresponding times.

The dissolution of I appears to have a slight dependency on the pH of the dissolution medium. This is more pronounced after the first 10 min of dissolution and is reflected in the LDC as shown in Table III. In all cases, except the 9:1 coprecipitate, the LDC is less at pH 5.0 than pH 2.0 which is consistent with other reports of the dissolution of griseofulvin coprecipitates at various pH values (4). However, the 9:1 coprecipitate displayed a reverse and significant pH dependency in its dissolution profile which is not readily explained. This result, together with the unusually greater LDC of the 4:1 coprecipitates, suggest that the physical characteristics of the crystals formed in the coprecipitates differ from sample to sample and are dependent on the proportions of I and II.

Solid-State Analysis—Differential thermal analysis (DTA) of I pretreated with chloroform yielded a sharp major endothermic peak at 221°C [lit. (4) mp 220–222°C]. However, a distinct, broad peak also occurred at 120–126°C.

[4] Mettler FP52, hot-stage microscope; Mettler Instrument Corp., Princeton, N.J.
[5] Fisher Thermalyzer, Model 370; Fisher Scientific Co., N.J.
[6] Calorimetric Standards; Fisher Scientific Co., N.J.
[7] Philips X-Ray Diffractometer, Model 1380, with a Norelco focusing monochromator.
[8] Magne-Drive Dissolution Test Apparatus; Clow-Coffman Industries, Kansas City, Kan.
[9] Zeiss standard microscope with integral 6-V 10-W halogen illuminator equipped with an MC63 photomicrographic camera; Carl Zeiss, Oberkochen, West Germany.
[10] Kodak Plus-X Pan Film, ASA 125, 1/15-s exposure.

Table II—Comparison of Percent Dissolved from Griseofulvin–Dimyristoylphosphatidylcholine Coprecipitates, Physical Mixtures, and Pure Griseofulvin

Composition (Weight Ratio)	Coprecipitates				Physical Mixtures			
	5 min	20 min	40 min	60 min	5 min	20 min	40 min	60 min
1:0	3.2	15.8	23.8	27.0	3.2	15.8	23.8	27.0
9:1	16.8	43.1	48.7	49.8	5.6	18.5	24.5	17.5
1.5:1	27.9	72.8	83.9	86.4	7.0	25.1	35.7	41.1

It also appeared in the thermograms of coprecipitates and physical mixtures, but its height varied in proportion to the I content of the sample. This peak did not appear in thermograms of I pretreated with methanol or acetone or untreated I. Chloroform solvates of I have been reported (11, 12) and, therefore, it is concluded that the unexpected peak was due to chloroform, in spite of fairly rigorous drying of each treated sample.

Thermograms of the binary systems contained two peaks: a peak corresponding to the melting of I and a peak corresponding to the melting of II. Determination of the thaw and melt temperatures from each peak enabled construction of the phase diagram (Fig. 2). The line for the solid indicates a slight depression of the melting point of II as the composition increases with respect to I. Likewise, the line for the liquid displays a slight decrease in the melting point of I as the composition decreases with respect to I. Hot-stage microscopy permitted visualization of the melting of each component and confirmed the thaw and melt temperatures. Above 70% II, the I peak on the DTA thermogram was too small to accurately measure, so hot-stage microscopy results are recorded only. The phase diagram is typical of a monotectic system (13), which indicates the absence of eutectic or solid solution formation. Thus, no strong interaction between I and II exists.

The relevant fusion temperatures and heats of fusion (ΔH_f) for systems examined for their dissolution behavior are given in Table IV. It can be seen that the fusion temperatures are similar for coprecipitates and physical mixtures, but the heats of fusion differ. There is a gradual and uniform decrease in ΔH_f with coprecipitate compositions, whereas an abrupt decrease in ΔH_f occurs with the 19:1 physical mixture; it remains essentially constant for all other compositions.

The dissolution studies demonstrated that the dissolution of I from the 19:1 coprecipitate was nearly as dramatic as from other coprecipitates containing a larger fraction of II (Table I). Thus, the physical state of the 19:1 composition was studied in detail in order to gain an insight into the mechanisms of dissolution of these systems. Several possibilities exist which may account for the increased dissolution of I–II coprecipitates. Therefore, X-ray diffraction spectra were prepared to attempt to resolve some of these issues. Typical X-ray diffraction patterns of powdered samples of II, chloroform-treated I, and the 19:1 coprecipitate are shown in Fig. 3. The crystalline properties of I are characterized by two major and four minor peaks in the spectrum, whereas the II spectrum displays the properties of an amorphous material. The identifiable peaks of I are also visible in the spectrum of the 19:1 coprecipitate even though there appears that some broadening and loss of detail of the peaks has occurred. The positions of the diffraction peaks of I were not altered compared with that of the pure compound. Physical mixtures and 19:1 coprecipitates all exhibited the identifiable peaks of I in their spectra 2 h, 1 week, and 2 weeks after preparation although there were variations in the shapes and intensities of the peaks. These clearly indicate that I does not exhibit polymorphism, complex formation, eutectic, or solid solution formation with II in the coprecipitate.

DISCUSSION

When the solid dispersion system has been employed to formulate drugs having low water solubility, invariably the inert carrier is one which either undergoes rapid dissolution (*e.g.*, urea, polyethylene glycol, or polyvinylpyrrolidone) to increase the dissolution of the drug (14) or it is one which undergoes slow dispersion in aqueous media to provide sustained release [*e.g.*, tristearin, cholesterol, or cholesteryl ester (3, 7)]. If the lipid has significant surface activity [*e.g.*, cholesteryl stearate (3) or polyoxyl 40 stearate (4)] usually an increase in dissolution of drug due to wetting is observed. Solubilization of the drug during dissolution may also play a role (4). Phospholipids have not previously been employed to prepare solid dispersions of drugs. Yet these nontoxic agents have the ability to both increase the wetting of hydrophobic drug particles and to spontaneously disperse into colloidal aggregates, with the capacity to sequester substantial quantities of drug in lipidic or aqueous compartments.

The best solid dispersion systems from the point of view of rapid release of drug have been those containing large ratios of carrier to drug (15), although compositions high in drug content have been chosen in some instances as

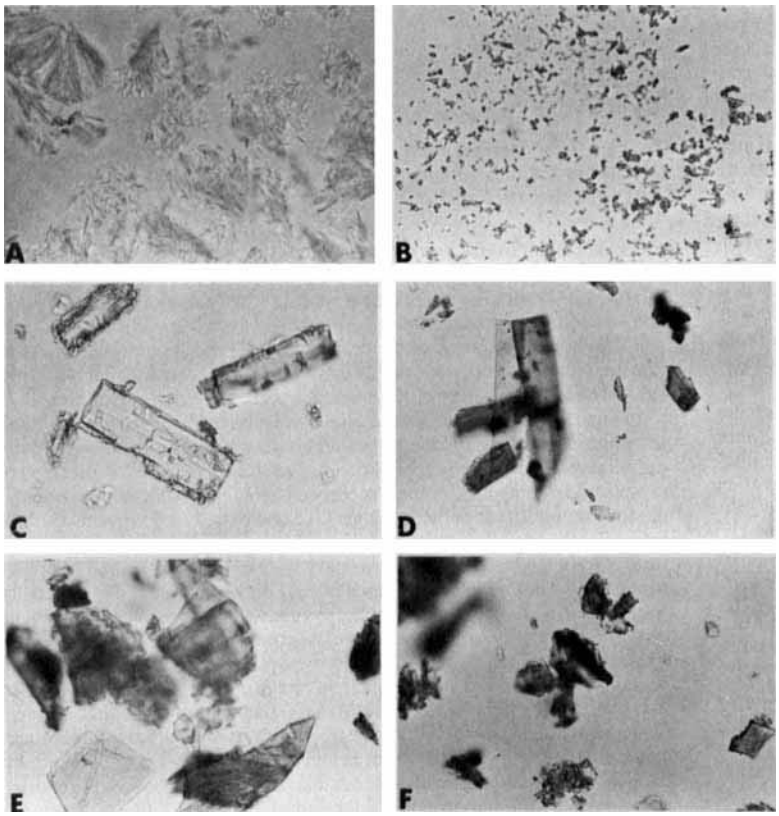

Figure 4—*Photomicrographs of various test samples dispersed in light mineral oil (320× magnification). Key: (A) untreated II; (B) untreated, micronized I; (C) chloroform-treated I; (D) 9:1 I–II coprecipitate; (E) 4:1 I–II coprecipitate; (F) 1.5:1 I–II coprecipitate.*

Table III—Effet of pH on the Dissolution of Coprecipitates of Griseofulvin and Dimyristoylphosphatidylcholine

Composition (Weight Ratio)	Initial Dissolution Rate, mg/L/min		Limiting Conc. After 60 min, mg/L	
	pH 2.0	pH 5.0	pH 2.0	pH 5.0
1:0	0.36	0.40	15.0	12.4
19:1	1.26	1.21	25.8	25.4
9:1	1.68	1.53	25.9	28.8
4:1	1.67	1.63	35.3	34.0
1.5:1	1.86	1.56	28.8	26.2

representing eutectic mixtures (16-18). However, it has now been demonstrated that high rates of dissolution are possible from coprecipitates with drug content as high as 95% using a phospholipid carrier. Furthermore, as the carrier content of the coprecipitate is increased, the IDR of I increases by a further 50%, while the apparent solubility of I at pH 2.0 (LDC) increases by a further 12%, following an 8-fold increase in the percentage of phospholipid in the sample (see Table I). Thus, unlike the griseofulvin-succinic acid solid dispersion (19), decreasing the carrier content, when it is phospholipid, does not necessarily result in the formation of larger crystals of I.

The X-ray diffraction spectra and the phase diagram for the I-II system clearly indicate the lack of any specific I-II interaction. This is substantiated by the observation that under the microscope crystals of I and I-II coprecipitates have approximately the same shape and size (Fig. 4C-F).

In view of the above discussion, there are two possible mechanisms which may be responsible for the greater dissolution behavior of coprecipitates than for pure drug or physical mixtures. In the first instance, it is reasonable to assume that on coprecipitation of I and II from chloroform, crystals are formed having mainly characteristics of chloroform-treated I, at least with medium to high I compositions. The chloroform solvate of I is an important factor in its physical state, as described earlier in the DTA results and previously by others (11, 12, 20). However, it would appear that the packing arrangement of the molecules in the coprecipitate crystal is different than in the absence of II, leading to a major change in the stabilization energy of the crystals. This packing arrangement would appear to be ideal for rapid release of I and its transfer from the solid state to the solution state. A good linear correlation was found between the percent of I dissolved and ΔH_f for coprecipitates ($r > 0.97$) at all dissolution times, but not with physical mixtures after 5 min. Furthermore, aging of the coprecipitates resulted in reduced dissolution rates, although X-ray diffraction patterns of aged samples were essentially unchanged. The dissolution behaviors of untreated micronized I, treated I, and aged treated I were essentially identical.

According to the film theory of dissolution (21) factors influencing the rate of dissolution include the diffusion coefficient, the stationary or diffusion layer thickness, the surface area, and the difference between the saturation concentration in the diffusion layer and the bulk solution concentration. Under identical conditions of dissolution testing for the same compositions of I-II, differences in dissolution behavior between coprecipitates and physical mixtures or pure drug are likely to originate from changes in the total surface area during the dissolution process and the diffusion layer concentration-bulk solution concentration difference at any given time. In the case of the coprecipitate, very fine crystallites of I may become available as the original crystals fracture and break up in the dissolution medium, thereby increasing the total surface area of I. The situation is obviously different with regard to the physical mixtures, where the phospholipid, which may not undergo rapid dispersion, provides very little wetting of the crystals of I and only a minor increase in the effective surface area. The result is a slight increase in the IDR as seen in Table I.

The solubilization effect in the diffusion layer surrounding the particles may be exerting the most substantial effect in the dissolution process. More specifically, it is the rapid, spontaneous dispersion of II into colloidal aggregates of phospholipid bilayers (liposomes) and the simultaneous incorporation

Table IV—Fusion Temperatures and Heats of Fusion of Griseofulvin and Griseofulvin-Dimyristoylphosphatidylcholine Compositions

Composition (Weight Ratio)	Fusion Temp., °C		ΔH_f, cal/g	
	Coprecipitates	Physical Mixtures	Coprecipitates	Physical Mixtures
1:0	221.8	221.8	28.4	28.4
19:1	219.0	219.3	25.7	19.7
9:1	217.0	218.8	24.0	19.6
4:1	217.4	216.0	20.8	19.3
1.5:1	215.3	214.5	18.2	20.5
0:1	67.9	67.9	17.1	17.1

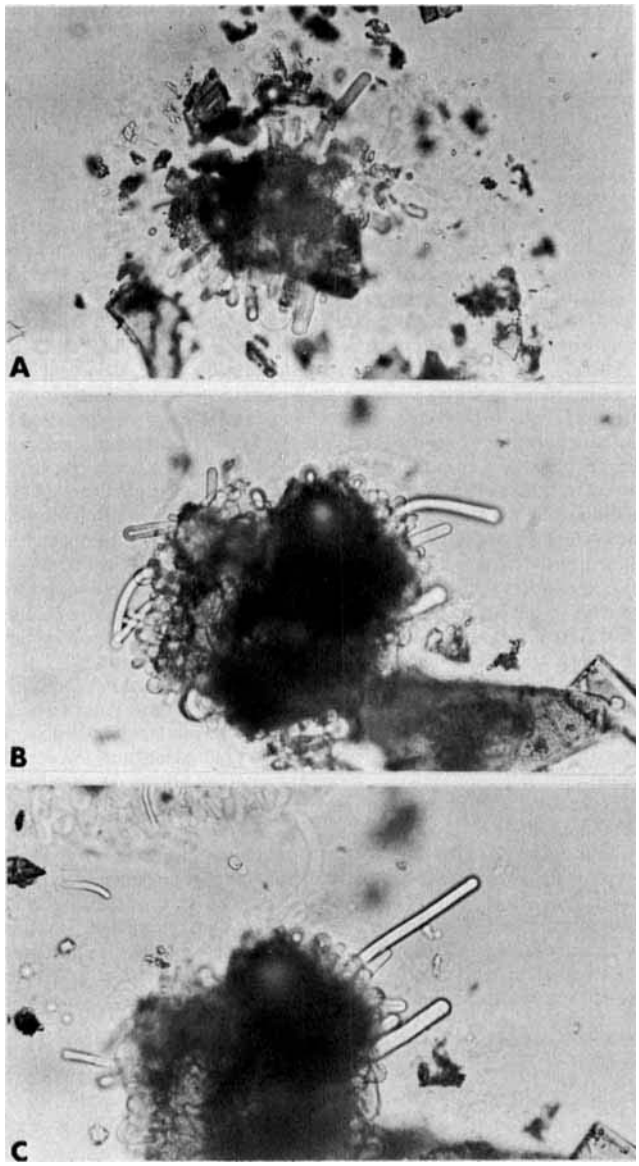

Figure 5—*Photomicrographs of 1.5:1 I-II coprecipitate crystals dispersed in water at various time periods after preparation (320× magnification) Key: (A) 2 min; (B) 3 min; (C) 5 min.*

of I molecules into this partitioning system that is analogous to an increase in the saturation concentration in the diffusion layer. In the case of physical mixtures, II is not in as desirable a physical state for spontaneous dispersion and, in addition, I molecules must be dissociated from the solid state by solvent and then become sequestered by the liposomes. The vigorous agitation of the dissolution medium coupled with its large volume decrease the chances of any substantial sequestering of I molecules adjacent to the particle surfaces.

In an attempt to determine the validity of this reasoning, microscopic observation of coprecipitate crystals undergoing dissolution in water was carried out. Figure 5 shows a sequence of photomicrographs of a 1.5:1 coprecipitate sample undergoing dissolution. As early as 2 min following mixing, it is apparent that multitudes of long, finger-like bodies (myelinic structures) had formed at the crystal surfaces. These could be seen as growing and extending further outward into the medium as part of a rapid, dynamic process of dispersion and what may be considered as part of the process of dissolution. It was interesting to note that a similar picture was observed when a physical mixture was examined, but the formation and dispersal of the myelinic structures was much slower. Although these observations are based on what must be considered as a static system, in relative terms, it demonstrates that phospholipids can play a role in solid dispersion formulations that is much different than that observed with other lipids or surfactants. Studies are continuing along these lines to determine the potential of phospholipids in developing formulations which have the dual roles of controlled release of drug and bioavailability improvement following oral administration.

REFERENCES

(1) D. C. Bloedow and W. L. Hayton, *J. Pharm. Sci.*, **65**, 328 (1976).
(2) K. Taniguchi, S. Muranishi, and H. Sezaki, *Int. J. Pharm.*, **4**, 219 (1980).
(3) K. H. Kim and C. I. Jarowski, *J. Pharm. Sci.*, **66**, 1536 (1977).
(4) R. Kaur, D. J. W. Grant, and T. Eaves, *J. Pharm. Sci.*, **69**, 1321 (1980).
(5) J. A. Grisafe and W. L. Hayton, *J. Pharm. Sci.*, **67**, 895 (1978).
(6) S. P. Patel and C. I. Jarowski, *J. Pharm. Sci.*, **64**, 869 (1975).
(7) K. S. Chang and C. I. Jarowski, *J. Pharm. Sci.*, **69**, 466 (1980).
(8) H. J. Borchart and F. Daniels, *J. Am. Chem. Soc.*, **79**, 41 (1957).
(9) A. C. Shah, C. B. Peot, and J. F. Ochs, *J. Pharm. Sci.*, **62**, 671 (1973).
(10) J. C. Wallach, *Pharm. Tech. Int.*, **3**, 34 (1980).
(11) M. Mayersohn and M. Gilbaldi, *J. Pharm. Sci.*, **55**, 1323 (1966).
(12) K. C. Cheng, E. Shefter, and T. Srikrishnan, *Int. J. Pharm.*, **2**, 81 (1979).
(13) R. Kaur, D. J. W. Grant, and T. Eaves, *J. Pharm. Sci.*, **69**, 1317 (1980).
(14) W. L. Chiou and S. Riegelman, *J. Pharm. Sci.*, **60**, 1281 (1971).
(15) A. P. Simonelli, S. C. Mehta, and W. I. Higuchi, *J. Pharm. Sci.*, **58**, 538 (1969).
(16) K. Sekiguchi, N. Obi, and Y. Ueda, *Chem. Pharm. Bull.*, **12**, 134 (1964).
(17) W. L. Chiou, *J. Pharm. Sci.*, **60**, 1406 (1971).
(18) J. A. Rogers and A. J. Anderson, *Pharm. Acta. Helv.*, **10–11**, 276 (1982).
(19) W. L. Chiou, *J. Pharm. Sci.*, **66**, 989 (1977).
(20) K. Sekiguchi, I. Horikoshi, and I. Himuro, *Chem. Pharm. Bull.*, **16**, 2495 (1968).
(21) J. T. Carstensen, in "Dissolution Technology," L. G. Leeson and J. T. Carstensen, Eds., Academy of Pharmaceutical Sciences, Washington, D.C., 1974, pp 1–28.

ACKNOWLEDGMENTS

Presented to the Basic Pharmaceutics Section at the 33rd National Meeting of the APhA Academy of Pharmaceutical Sciences, San Diego, Calif., November 1982.

The award of an Alberta Heritage Foundation for Medical Research Studentship to S.V. is greatly appreciated. A gift of griseofulvin from Glaxo Canada Ltd. is kindly acknowledged. The X-ray diffraction spectra were carried out in the Department of Mineral Engineering, University of Alberta, with the generous cooperation of Dr. S. Bradford and the expert technical assistance of Mrs. T. Parker.

Model-Independent Steady-State Plasma Level Predictions in Autonomic Nonlinear Pharmacokinetics I: Derivation and Theoretical Analysis

PETER VENG-PEDERSEN

Received January 17, 1983, from the *Divison of Pharmacokinetics, School of Pharmacy and Pharmacal Sciences, Purdue University, West Lafayette, IN 47907.* Accepted for publication May 21, 1983.

Abstract □ Current drug level predictions in nonlinear pharmacokinetics are based on specific pharmacokinetic models in contrast to the model-independent (structureless), dose-linearity, and superposition principles used in linear pharmacokinetics. Such model-dependent methods may not provide reliable predictions due to their inherent nonuniqueness, computational complexity, and often unrealistic kinetic assumptions. Some novel model-independent methods for predicting the steady-state drug levels of extravascular, intravenous bolus, and intravenous infusion administrations are presented that should overcome such disadvantages. The methods only assume an autonomic nonlinear kinetic behavior, which implies that following an intravenous bolus administration the derivatives of the drug concentration–time profile at arbitrary drug levels are independent of the dose given. Such a kinetic behavior is found for any nonlinear pharmacokinetic system when the rate of change of the drug level following an intravenous bolus administrations depends only on the drug level, *i.e.*, $dC/dt = -q(C)$, where q can be any function dependent only on C and time-invariant kinetic parameters. The basic approach presented represents a novel alternative which avoids the very difficult and often impractical task of identifying and incorporating the numerous kinetic parameters and processes responsible for the observed drug concentration data into a useful pharmacokinetic model. The focus in the kinetic analysis is instead on two much simpler processes: (*a*) fitting empirical functions to estimate the mean drug disposition behavior of the subject or population and (*b*) testing the validity of the assumptions involved.

Keyphrases □ Pharmacokinetics—nonlinear, model independent, steady-state plasma drug-level predictions, theory and mathematical models □ Plasma drug levels—prediction at steady state, model-independent nonlinear pharmacokinetics, theory and mathematical models

Steady-state plasma level predictions in linear pharmacokinetics are done by extrapolations using the dose-linearity and superposition principles or by using the convolution property of linear pharmacokinetics. The plasma level profiles used for the predictions are most commonly determined by fitting suitable model-independent[1] equations, typically of an exponential type, to available plasma level data. Such model-independent methods cannot be used for drugs showing nonlinear pharmacokinetics because the superposition and dose-linearity principles do not apply. Consequently, drug level predictions in nonlinear pharmacokinetics have been based on model-dependent methods, which may not provide reliable predictions due to their inherent nonuniqueness, computational complexity, and often unrealistic model assumptions. A model-independent approach is presented which overcomes some of these disadvantages.

THEORETICAL

The proposed methodology applies to drugs showing what will be called *autonomic nonlinear pharmacokinetics; i.e.*, the drug-concentration profile resulting from an intravenous bolus dose adheres to the autonomic differential equation:

$$\frac{dC}{dt} = -q(C) \qquad \text{(Eq. 1)}$$

where q stands for any function only dependent on the drug concentration C and time-invariant kinetic parameters. It is assumed that q is such that the solution of Eq. 1, $C(t)$, is monotonically decreasing with time. Autonomic nonlinear pharmacokinetics is readily identified in a model-independent manner from "the horizontal superposition property" (Fig. 1). Different intravenous bolus doses result in drug-concentration profiles with identical slopes

[1] The terminology "model-independent" is used here to denote a general approach not based on a specific structured (model-dependent) kinetic analysis of the individual kinetic components of the pharmacokinetics.

0022-3549/84/0600-0761$01.00/0